

2014

## New Insights into the Mechanism of Visible Light Photocatalysis

Suresh Pillai

*Technological University Dublin, suresh.pillai@tudublin.ie*

Swagata Banerjee

*Technological University Dublin*

Polycarpos Falaras

*Institute of Advanced Materials, Athens Greece.*

*See next page for additional authors*

Follow this and additional works at: <https://arrow.tudublin.ie/ehsiart>

 Part of the [Physical Sciences and Mathematics Commons](#)

### Recommended Citation

Pillai, S. et al. (2014). New Insights into the Mechanism of Visible Light Photocatalysis. *Journal of physical chemistry letters Letters*. Vol. 5, No. 15, 2014, pp 2543–2554. doi:10.1021/jz501030x

This Article is brought to you for free and open access by the ESHI Publications at ARROW@TU Dublin. It has been accepted for inclusion in Articles by an authorized administrator of ARROW@TU Dublin. For more information, please contact [arrow.admin@tudublin.ie](mailto:arrow.admin@tudublin.ie), [aisling.coyne@tudublin.ie](mailto:aisling.coyne@tudublin.ie).



This work is licensed under a [Creative Commons Attribution-Noncommercial-Share Alike 4.0 License](#)

---

**Authors**

Suresh Pillai, Swagata Banerjee, Polycarpos Falaras, Kevin O'Shea, John A. Byrne, and Dionysios D. Dionysiou

## New Insights into the Mechanism of Visible Light Photocatalysis

Swagata Banerjee,<sup>†</sup> Suresh C. Pillai,<sup>\*,‡,§</sup> Polycarpus Falaras,<sup>||</sup> Kevin E. O'Shea,<sup>⊥</sup> John A. Byrne,<sup>#</sup> and Dionysios D. Dionysiou<sup>\*,||</sup>

<sup>†</sup> Centre for Research in Engineering Surface Technology (CREST), FOCAS Institute, Dublin Institute of Technology, Kevin St, Dublin 8, Ireland

<sup>‡</sup> Department of Environmental Science, Institute of Technology Sligo, Sligo, Ireland

<sup>§</sup> Centre for Precision Engineering, Materials and Manufacturing Research (PEM), Institute of Technology Sligo, Sligo, Ireland

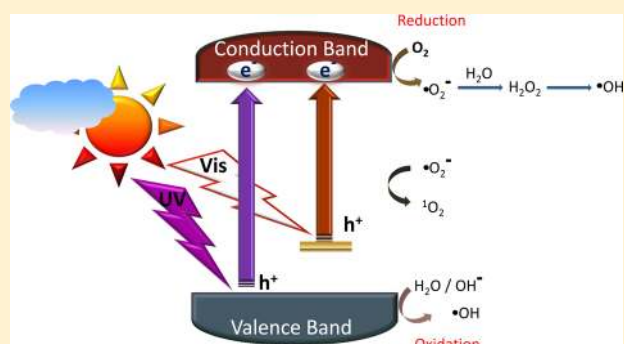
<sup>||</sup> Institute of Advanced Materials, Physicochemical Processes, Nanotechnology and Microsystems, NCSR Demokritos, Agia Paraskevi Attikis, P.O. Box 6003, 15310 Athens, Greece

<sup>⊥</sup> Department of Chemistry and Biochemistry, Florida International University, Miami, Florida 33199, United States

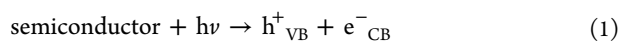
<sup>#</sup> Nanotechnology and Integrated Bio-Engineering Centre, School of Engineering, Faculty of Computing and Engineering, University of Ulster, Newtownabbey, Northern Ireland BT37 0QB, United Kingdom

<sup>||</sup> Environmental Engineering and Science Program, School of Energy, Environmental, Biological, and Medical Engineering, University of Cincinnati, Cincinnati, Ohio 45221-0012, United States

**ABSTRACT:** In recent years, the area of developing visible-light-active photocatalysts based on titanium dioxide has been enormously investigated due to its wide range of applications in energy and environment related fields. Various strategies have been designed to efficiently utilize the solar radiation and to enhance the efficiency of photocatalytic processes. Building on the fundamental strategies to improve the visible light activity of TiO<sub>2</sub>-based photocatalysts, this Perspective aims to give an insight into many contemporary developments in the field of visible-light-active photocatalysis. Various examples of advanced TiO<sub>2</sub> composites have been discussed in relation to their visible light induced photoconversion efficiency, dynamics of electron–hole separation, and decomposition of organic and inorganic pollutants, which suggest the critical need for further development of these types of materials for energy conversion and environmental remediation purposes.

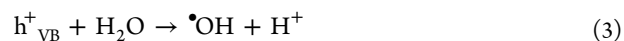


Photocatalysis widely refers to the process of using light to activate a substrate (photocatalyst), which modifies or facilitates the kinetics of a chemical reaction but itself remains unconsumed.<sup>1–4</sup> During photocatalysis, a semiconductor metal oxide such as titanium dioxide (TiO<sub>2</sub>) or zinc oxide (ZnO) is irradiated with light (where, the energy of the excitation source is higher than the band gap energy of the material), which results in photon absorption and excitation of an electron (e<sup>−</sup>) from valence band to the conduction band, thereby generating a positive electron hole (h<sup>+</sup>) in the valence band (Figure 1). The electron–hole charge carriers (h<sup>+</sup><sub>VB</sub> + e<sup>−</sup><sub>CB</sub>) can in turn undergo recombination and dissipate the excess energy through nonradiative mechanisms (eqs 1 and 2)



This reduces the overall efficiency of the photoinduced process. The charge carriers, which do not undergo charge annihilation, can migrate to the surface of the catalyst and initiate secondary reactions with the surface adsorbed materials.

For example, the photoexcited electron in the conduction band can react with oxygen to form superoxide radicals or hydroperoxide radicals and these reactive oxygen species (ROS) can participate in the degradation of organic pollutants, whereas positive holes (h<sup>+</sup>) in the valence band can oxidize surface adsorbed water or OH<sup>−</sup> and generate hydroxyl radical (•OH), which in turn oxidizes the organic pollutants (Figure 1; eqs 3 and 4).



Titanium dioxide (TiO<sub>2</sub>)-based materials have received enormous attention in the area of semiconductor photocatalysis. The major breakthrough came in the year 1972, when Fujishima and Honda demonstrated for the first time the

Received: May 22, 2014

Accepted: July 10, 2014

Published: July 10, 2014

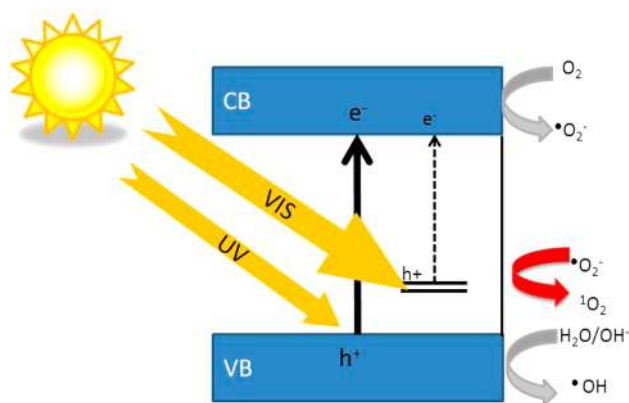


**Figure 1.** Schematic of semiconductor photocatalysis (adapted from ref 4). Copyright 2013, reprinted with permission from Elsevier.

photoelectrochemical decomposition of water using  $\text{TiO}_2$  as an anode and platinum as a counter electrode.<sup>5</sup>  $\text{TiO}_2$ -based photocatalysts also offer the advantages of high physical and chemical stability, low cost, easy availability, low toxicity, and excellent photoactivity. Titanium dioxide exists in three naturally occurring polymorphic forms such as anatase, rutile, and brookite, where rutile represents the thermodynamically stable form and anatase shows higher kinetic stability. The anatase form of  $\text{TiO}_2$  is reported to show higher photocatalytic activity compared to rutile or brookite.<sup>1,3</sup> The major drawbacks

The major drawbacks of  $\text{TiO}_2$ -based photocatalysts arise from the rapid charge recombination of the electron–hole pairs, thereby suppressing the quantum efficiency, and the wide band gap (3.0 eV for rutile and 3.2 eV for anatase) of the material, which restricts light absorption to only ultraviolet region (wavelength <390 nm) and thus limits the practical applications of  $\text{TiO}_2$ -based photocatalysts for solar light harvesting.

of  $\text{TiO}_2$ -based photocatalysts arise from the rapid charge recombination of the electron–hole pairs, thereby suppressing the quantum efficiency, and the wide band gap (3.0 eV for rutile and 3.2 eV for anatase) of the material, which restricts light absorption to only ultraviolet region (wavelength <390 nm) and thus limits the practical applications of  $\text{TiO}_2$ -based photocatalysts for solar light harvesting. Various strategies including dye sensitization,<sup>6–9</sup> metal,<sup>10–14</sup> or nonmetal doping<sup>15–17</sup> have been developed to improve the visible light activity (VLA) of  $\text{TiO}_2$  in order to use the solar irradiation or interior lighting efficiently.

Chemical modifications of  $\text{TiO}_2$  lattice using nonmetals such as C,<sup>18–23</sup> N,<sup>24–26</sup> and S<sup>27–29</sup> appeared as promising strategies to improve visible light responsive photocatalytic activity. In 1986, Sato reported that the incorporation of ammonium hydroxide in a titania precursor sol, followed by a calcination

process, resulted in a nitrogen-doped photocatalyst that demonstrated visible light activity.<sup>30</sup> Asahi and co-workers further showed that nitrogen-doped  $\text{TiO}_2$  exhibit a substantial enhancement in visible light assisted photocatalytic degradation of methylene blue and acetaldehyde compared to undoped  $\text{TiO}_2$ .<sup>31</sup> Following this work, various research groups have designed visible-light-active N-doped  $\text{TiO}_2$  photocatalysts. Incorporation of nitrogen into  $\text{TiO}_2$  lattice is favored due to comparable atomic sizes of nitrogen and oxygen, low ionization potential, and high stability of nitrogen.<sup>25,26,32</sup> Although nonmetal doping (e.g., N, C, F, S, etc.) is found to shift the absorption band of  $\text{TiO}_2$  towards the visible region, the chemical nature of the doped species accountable for the visible light activity and the electronic structure of the doped material still remain controversial. In their pioneering work, Asahi and co-workers proposed that substitutional N doping results in band gap narrowing due to efficient mixing of 2p orbitals of N and O. Contrary to this, Serpone and co-workers argued that observations of band gap narrowing through modifications in the energy levels of valence and conduction bands requires high concentrations of dopants and strong interactions among impurity energy states, valence, and conduction bands.<sup>32</sup>

Serpone et al., also suggested that the presence of defects (color centers) associated with oxygen vacancies in doped  $\text{TiO}_2$  are responsible for their visible light activity.<sup>32</sup> Di Valentin and co-workers showed the electronic nature of the N-dopant in  $\text{TiO}_2$  synthesized through various chemical routes.<sup>33–36</sup> Density functional theory (DFT) predicted that the doped N atoms could occupy substitutional or interstitial sites in the  $\text{TiO}_2$  lattice and generate localized energy levels in the band gap. For dopants occupying substitutional positions, a continuum of slightly higher energy levels essentially extends the valence band, whereas an interstitial dopant results in discrete energy levels above the valence band, often referred to as a midgap state (Figure 2A).<sup>35,36</sup> The visible light response in the doped materials arises from the electron transition from the localized N orbitals to the conduction band or to the surface adsorbed  $\text{O}_2$ .<sup>36</sup> Doping  $\text{TiO}_2$  with carbon or sulfur also is found to enhance visible light activated photocatalytic activity.<sup>15,22</sup> The visible light response in these doped materials is thought to arise from the presence of localized energy levels of the dopant lying above the valence band or oxygen vacancies as demonstrated in Figure 2.<sup>23</sup> It was also reported that in case of substitutional doping of  $\text{TiO}_2$  by lighter elements such as N, C, and B, the dopant with lower atomic number will appear at higher energy in the band gap due to smaller effective nuclear charge.<sup>33</sup> Visible-light-active, oxygen-rich  $\text{TiO}_2$  that exhibits anatase phase stability up to 900 °C, suitable for high temperature applications, has also been developed.<sup>37</sup> The visible light response in the oxygen rich  $\text{TiO}_2$  arises from the band gap narrowing of  $\text{TiO}_2$  containing oxygen excess defects, which can interact with the lattice oxygen atoms, thereby increasing lattice parameters and consequently decrease the band gap.<sup>37</sup>

In order to improve the visible-light-active photocatalytic efficiency and inhibit charge recombination, several research groups have developed  $\text{TiO}_2$  composites codoped with two or more nonmetals such as S–N,<sup>38</sup> B–N,<sup>39</sup> C–N,<sup>40,41</sup> N–F,<sup>42–47</sup> in  $\text{TiO}_2$ . Hamilton et al. recently reported using photoelectrochemistry in N and F codoped  $\text{TiO}_2$  that electrons could be promoted from nitrogen centers (which are located just above the valence band) directly to the conduction band by visible light.<sup>48</sup> It was also showed that the vacant N states thus

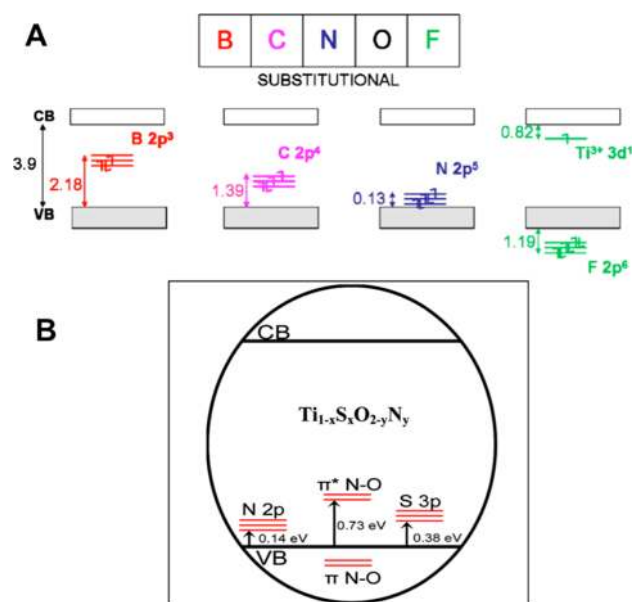


**Figure 2.** (A) Schematic illustration of localized impurity energy states for the substitutionally doped  $\text{TiO}_2$  (adapted from ref 33). Copyright 2013, reprinted with permission from Elsevier. (B) Electronic structure of  $\text{Ti}_{1-x}\text{S}_x\text{O}_{2-y}\text{N}_y$ , showing the presence of localized impurity energy states (adapted from ref 73). Copyright 2012, reprinted from with permission from American Chemical Society.

The visible light response in the doped materials arises from the electron transition from the localized N orbitals to the conduction band or to the surface adsorbed  $\text{O}_2$ .<sup>36</sup> Doping  $\text{TiO}_2$  with carbon or sulfur also is found to enhance visible light activated photocatalytic activity.<sup>15,22</sup> The visible light response in these doped materials is thought to arise from the presence of localized energy levels of the dopant lying above the valence band or oxygen vacancies.

produced could be refilled by electron transfer from  $\text{Ti}^{3+}$  states, which could further accept conduction band electrons. Oxygen vacancies ( $\text{O}_{\text{vac}}$ ) situated just above the nitrogen midgap state could also transfer electrons to refill the empty N states. The conduction band electrons can then donate electrons to the oxygen vacancy sites. Therefore, a cycle of events of excited electrons occurs from the N midgap state, to the conduction band, and then to  $\text{Ti}^{3+}$  or  $\text{O}_{\text{vac}}$  with eventual repopulation of the excited empty nitrogen states as demonstrated in (Figure 3).<sup>48</sup>

In a recent study, Zhao et al. showed that N–F codoped  $\text{TiO}_2$  exhibited the best performance to destroy 6-hydroxymethyl uracil (6-HOMU), a model compound for cyanotoxins.<sup>47</sup> Mechanistic investigations carried out in the presence of scavengers for  $\cdot\text{O}_2^-$ ,  $^1\text{O}_2$ ,  $\cdot\text{OH}$ , and  $\text{h}^+_{\text{vb}}$  have shown that  $\cdot\text{O}_2^-$

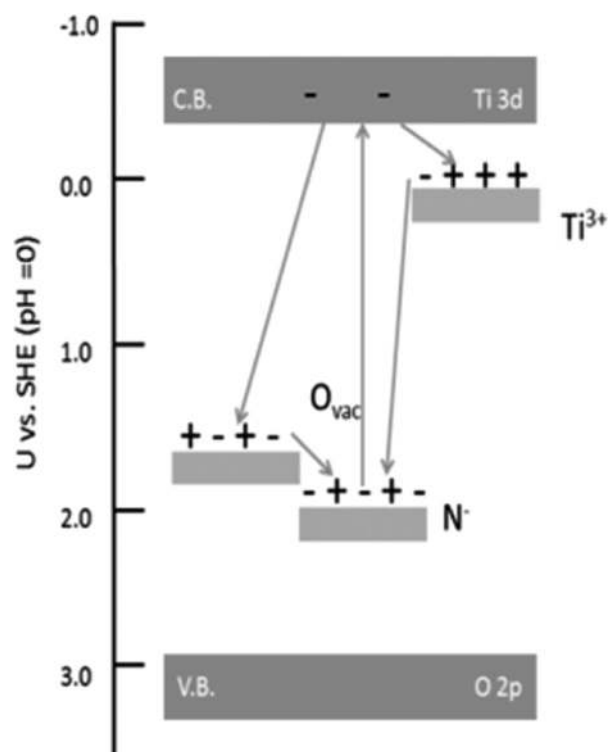


**Figure 3.** Visible light excitation of N–F codoped  $\text{TiO}_2$  and refilling of empty N states by electron transfer from either  $\text{Ti}^{3+}$  or  $\text{O}_{\text{vac}}$  (adapted from ref 48). Copyright 2014, reprinted with permission from American Chemical Society.

is the prime ROS leading to the photoassisted degradation of 6-HOMU (Figure 4). This study has contributed to the better basic understanding of different roles of ROS in doped and codoped visible-light-active titanium dioxide photocatalysts.<sup>47</sup> Pulgarin and co-workers suggested that for N,S codoped  $\text{TiO}_2$ , photogenerated holes formed under visible light irradiation do not possess suitable reduction potential to generate  $\cdot\text{OH}$  radical by the oxidation of  $\text{H}_2\text{O}$ .<sup>49,50</sup> It has also been reported that under visible light irradiation, less oxidative superoxide radical anion  $\cdot\text{O}_2^-$ , and singlet oxygen  $^1\text{O}_2$  species (Figure 1) are predominantly responsible for the photocatalytic bacterial inactivation.<sup>49,50</sup> However, under UV light excitation, highly oxidizing  $\cdot\text{OH}$  radicals are produced, which play active roles toward photocatalytic activity.<sup>49,50</sup>

Based on the first principle calculations (DFT), Huang and co-workers demonstrated that the presence of doping agents result in surface distortions in a  $\{101\}$  surface of  $\text{TiO}_2$ , which promotes transfer of photogenerated electrons from the bulk/subsurface atomic layer to the outer surface region, thereby facilitating the photocatalytic reactions and also improving quantum efficiency of photocatalytic processes by increasing the separation of photogenerated electrons and holes.<sup>51</sup> A gel combustion method has been recently developed to synthesize nanostructured modified  $\text{TiO}_2$  ( $\text{m-TiO}_2$ ) that involved calcination of a mixture of urea with an acidified solution of titanium alkoxide at temperatures 350–500 °C.<sup>52</sup> The hybrid inorganic/organic materials show unique physicochemical properties and remarkably high rate for visible light induced photocatalytic decomposition of methylene blue dye compared to the reference material Degussa (Evonik) P25. The significantly high visible light assisted photocatalytic activity of  $\text{m-TiO}_2$  materials with a core–shell morphology arises from

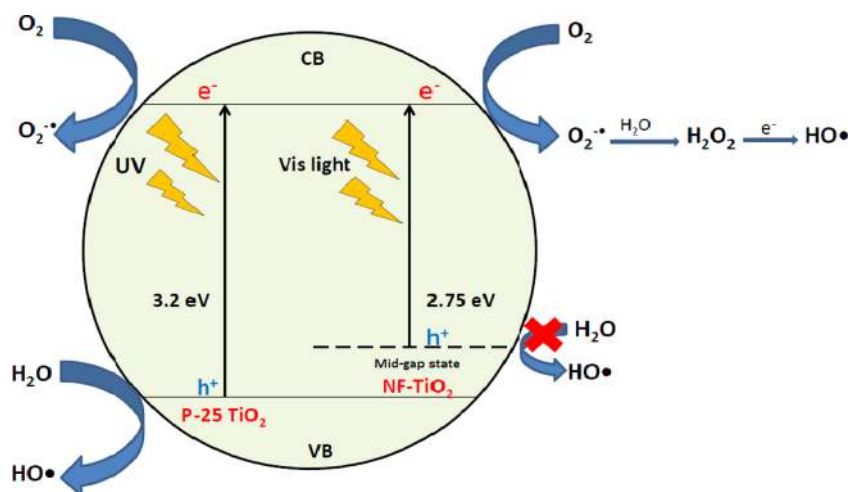


**Figure 4.** Production of different ROS during the visible-light-active photocatalytic processes for the destruction of 6-hydroxymethyl uracil (adapted from ref 47). Copyright 2014, reprinted with permission from Elsevier.

the sensitization of the  $\text{TiO}_2$  by a thin porous layer of carbonaceous species, which also favors charge separation and impede charge recombination at the inorganic/organic heterojunction.<sup>52</sup>

Chemical modifications of  $\text{TiO}_2$  with 3d transition metal ions,<sup>10,53</sup> lanthanides,<sup>13,14</sup> and noble metals<sup>54–56</sup> have also been found to improve the visible light response of  $\text{TiO}_2$ . It was shown that the addition of increased amounts of Ag up to 5 mol % facilitates visible light absorbance.<sup>57</sup> Many different explanations have been proposed to account for the enhanced visible light activity of such doped  $\text{TiO}_2$ , including band gap narrowing, formation of impurity energy levels within the band gap of  $\text{TiO}_2$ , and formation of intrinsic defects (such as oxygen vacancies, interstitial Ti). However, addition of metal ion impurities can also induce recombination of charge carriers and lower the overall efficiency of photocatalysis.  $\text{TiO}_2$  photocatalyst surface modified with  $\text{Rh}^{3+}$  has displayed very high activity for mineralization of volatile organic compounds (VOC) under visible light irradiation compared to conventional metal doped  $\text{TiO}_2$ .<sup>58</sup> The enhanced activity of  $\text{Rh}^{3+}$ -modified  $\text{TiO}_2$  has been attributed to the bifunctional role of  $\text{Rh}^{3+}$  as an electron injector as well as a promoter for multielectron reduction of  $\text{O}_2$  under visible light irradiation. Electron transfer occurs from the  $d$  orbital of  $\text{Rh}^{3+}$  to the conduction band of  $\text{TiO}_2$  under visible light irradiation, thereby forming  $\text{Rh}^{4+}$ , which in turn participates in degradation of organic substrate and undergoes reduction to  $\text{Rh}^{3+}$  species (Figure 5). Electrons in the conduction band of  $\text{TiO}_2$  can be transferred to  $\text{O}_2$  to

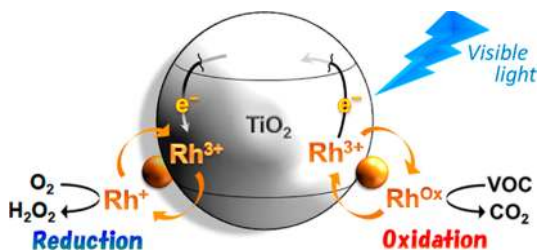


**Figure 5.** Schematic representation showing the dual role of  $\text{Rh}^{3+}$  in Rh modified  $\text{TiO}_2$  as an electron injector as well as a promoter for two electron reduction of  $\text{O}_2$  (ref 58). Copyright 2013, reprinted with permission from American Chemical Society.

form  $\text{O}_2^{\bullet -}$  through one electron reduction mechanism. Alternatively,  $\text{Rh}^{3+}$  can function as a conduction band electron acceptor to yield unstable  $\text{Rh}^{2+}$ , which rapidly forms  $\text{Rh}^+$ , a species capable of reducing  $\text{O}_2$  to  $\text{H}_2\text{O}_2$  through two electron transfer reduction and thus acts as a promoter for  $\text{O}_2$  reduction.

In recent years incorporation of plasmonic noble metal nanostructures appear as an attractive approach to enhance the visible light absorption due to direct excitation of the surface plasmon resonance (SPR) band of the nanoparticles.<sup>59,60</sup> Plasmonic nanostructures are being increasingly used to enhance the light harvesting efficiency of photovoltaic devices.<sup>61–64</sup> For example, Kamat and co-workers demonstrated that the photocurrent generation of nanostructured  $\text{TiO}_2$  films increases several times in the presence of surface deposited gold nanoparticles, which promote charge transfer process in the composite systems.<sup>62,63</sup> In the presence of photoexcited plasmonic nanoforms, electron injection occurs from the nanosurface to the conduction band of  $\text{TiO}_2$  in femtosecond time scale (Figure 6).<sup>65</sup> The positive hole formed

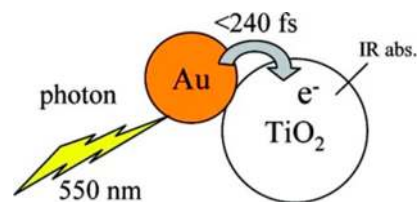


**Figure 6.** Schematic presentation showing electron injection from photoexcited Au to the conduction band of  $\text{TiO}_2$  in response to visible light absorption (ref 65). Copyright 2007, reprinted with permission from American Chemical Society.

on the nanosurface oxidizes the substrate, whereas the electron in the conduction band of  $\text{TiO}_2$  reacts further with  $\text{O}_2$ . However, the rapid back electron transfer and consequent charge recombination limit the efficiency of the photocatalytic processes. The size and shape of the metallic nanoparticles have significant effect on the overall efficiency of the process. Kamat and co-workers demonstrated that small sized nanoparticles shift the energy of the Fermi level of the  $\text{TiO}_2$ -nanocomposite toward more negative value and affect the photocatalytic process due to direct changes in the energetics of the composite systems.<sup>64</sup> Various mechanisms have been proposed to account

for the improved photocatalytic efficiency of TiO<sub>2</sub>-SPR nanostructures, including enhanced light absorption by the surface plasmons, improved charge separation efficiency, and changes in the energetics of the Fermi level in the composite system arising from the electron storage effects.<sup>66</sup> Alloying noble metal Cu with Pt (Pt-Cu) supported on anatase TiO<sub>2</sub> has resulted in a lower work function of metallic platinum, which in turn facilitates the efficient electron injection from the photoexcited platinum nanoparticles to the conduction band of TiO<sub>2</sub> due to lowering the height of Schottky barrier at the interface.<sup>67</sup> The Pt-Cu/TiO<sub>2</sub> catalyst exhibited high rate of alcohol oxidation under sunlight irradiation compared to Pt/TiO<sub>2</sub> composite.

Formation of TiO<sub>2</sub> with oxygen vacancy along with deposition of noble metal nanoparticle on such TiO<sub>2</sub> has been found to boost the photocatalytic performance.<sup>68</sup> Degussa (Evonik) P25 with oxygen vacancies was prepared through a photocatalytic reaction utilizing the oxidation of benzyl alcohol on TiO<sub>2</sub> surface, which creates oxygen vacancies. This was followed by the deposition of noble metal nanoparticles (Ag, Pt, Pd) on Degussa (Evonik) P25 with oxygen vacancy. The oxygen vacancy sites facilitate visible light absorption and electron-hole pair formation, whereas the metal nanoparticles can act as electron acceptors and promote interfacial charge separation and increase the lifetime of the charge separated species.

Formation of photocatalytic heterostructures based on TiO<sub>2</sub> with other semiconductor/noble metal has emerged as an important strategy to increase the separation of charge carriers and suppress the recombination rate of photoinduced electron-hole pair, resulting in improved photocatalytic efficiency.

In recent years, formation of photocatalytic heterostructures based on TiO<sub>2</sub> with other semiconductor/noble metal has emerged as an important strategy to increase the separation of charge carriers and suppress the recombination rate of photoinduced electron-hole pair, resulting in improved photocatalytic efficiency (Figure 7).<sup>69-74</sup> Additionally, the synergistic effects induced by the components in the heterostructure also result in an increased photostability and photocatalytic efficiency. Over the past decade, heterojunctions based on ZnO/TiO<sub>2</sub> nanocomposites,<sup>69</sup> anatase-rutile TiO<sub>2</sub> heterojunctions,<sup>70-73</sup> and Ag/TiO<sub>2</sub> nanofibers<sup>74</sup> have been developed for the degradation of organic pollutants and water splitting under UV-vis irradiation. Metallic oxides with oxygen vacancies such as W<sub>18</sub>O<sub>49</sub> are gaining huge interest in the field of visible light driven photocatalysis as they exhibit wide absorption tail in Near-Infrared (NIR) region arising from oxygen defects. Therefore, combination of TiO<sub>2</sub> with W<sub>18</sub>O<sub>49</sub> can result in a hybrid photocatalyst covering both UV and visible region.<sup>75</sup> Additionally such hybrid structures also favor enhanced photoinduced charge separation and inhibit charge recombination. It was found that simultaneous modification of TiO<sub>2</sub> with a nonmetal boron and nickel oxide (Ni<sub>2</sub>O<sub>3</sub>)

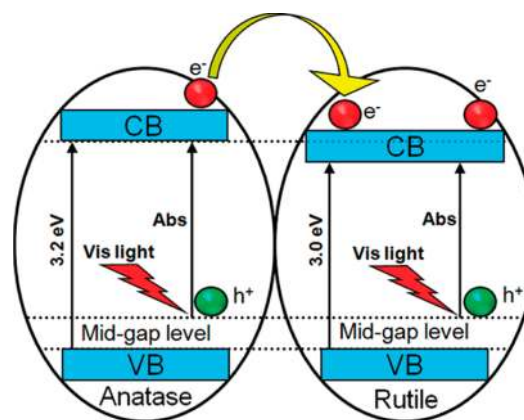


**Figure 7.** Electron transfer mechanism of anatase-rutile heterojunctions in visible light photocatalysts (ref 73). Copyright 2012, reprinted with permission from American Chemical Society.

significantly enhanced the photocatalytic activity of TiO<sub>2</sub> in the visible region and resulted in an efficient degradation of organic pollutants such as sodium benzoate, trichlorophenol, and 2,4-dichlorophenol.<sup>76</sup> Visible light irradiation of the modified photocatalyst using a Nd:YAG laser ( $\lambda = 532$  nm), generated long-lived charge carriers that can react with surface adsorbed O<sub>2</sub>/H<sub>2</sub>O to produce  $\cdot\text{OH}$  and  $\cdot\text{O}_2^-$  radicals, and promote mineralization of organic pollutants.<sup>76</sup> It has been proposed that Ni<sub>2</sub>O<sub>3</sub> loaded on the surface of B-doped TiO<sub>2</sub> acts as an electron trap and promotes charge separation.

Near-infrared light active core-shell TiO<sub>2</sub> nanoparticles were synthesized, where upconverting luminescent material (YF<sub>3</sub> codoped with Yb<sup>3+</sup>/Tm<sup>3+</sup> codoped) is used as the core and TiO<sub>2</sub> as the shell.<sup>77,78</sup> During the photoexcitation process, Yb<sup>3+</sup> absorbs NIR radiation and transfer the energy to Tm<sup>3+</sup>, which emits UV radiation and in turn excites TiO<sub>2</sub> to generate photoexcited electrons and holes. To further enhance the photocatalytic efficiency of these systems, nanocrystals of TiO<sub>2</sub> and a narrow-band semiconductor such as CdS were linked with NaYF<sub>4</sub> codoped with Yb<sup>3+</sup> and Tm<sup>3+</sup>.<sup>78</sup> Upon NIR excitation, Yb<sup>3+</sup> acts as a sensitizer and transfers the energy to Tm<sup>3+</sup>, which in turn activates CdS or TiO<sub>2</sub> by Förster resonance energy transfer or photon reabsorption mechanism and generates photoinduced electron and hole required for mineralization of organic chemicals. The presence of CdS/TiO<sub>2</sub> heterojunction further enhances the photocatalytic efficiency by facilitating the separation and migration of charge carriers at the interface.

Advanced nanostructured photocatalytic materials have been synthesized by combining TiO<sub>2</sub> nanoparticles with reduced graphene oxide (r-GO)<sup>79-83</sup> and carbon nanotube (CNT)<sup>80</sup> using liquid phase deposition method followed by thermal reduction at different temperatures. VLA nanocatalysts and composite materials were immobilized onto hybrid ultra/nanofiltration membranes (with improved permeability and low energy consumption) and incorporated into state of the art photocatalytic reactors, where the nanocomposites were systematically evaluated for their ability to degrade a number of pollutants under both UV and visible light irradiation.<sup>81-83</sup>

Dye sensitization is also considered to be a promising strategy to induce visible light activated photocatalysis by TiO<sub>2</sub>.<sup>8-8</sup> The process involves light absorption (mainly visible light) by a transition metal complex or an organic dye (or a colored pollutant) known as sensitizer followed by electron

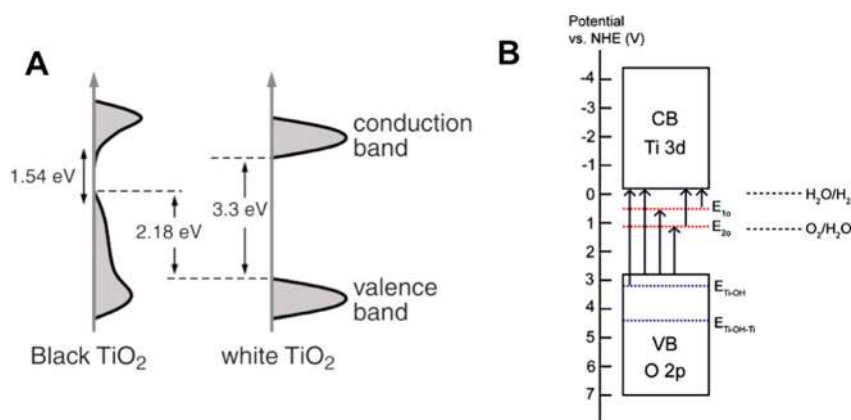


**Figure 8.** (A) Schematic representation showing the density of states of black  $\text{TiO}_2$  and white  $\text{TiO}_2$  nanocrystals (ref 90). Copyright 2011, reprinted with permission from Science. (B) Energy diagram of reduced  $\text{TiO}_2$  nanowires, where  $E_{10}$  and  $E_{20}$  shown in red dashed lines refer to the oxygen vacancies located at 0.73 and 1.18 eV below the  $\text{TiO}_2$  conduction band. Arrows represent electronic transitions between different energy levels (ref 91). Copyright 2011, reprinted with permission from American Chemical Society.

injection from the excited sensitizer molecule into the conduction band of semiconductor material. The resulting radical cations can lead to a number of oxidative processes and the formation of ROS leading to the degradation of target compounds such as various organic pollutants.<sup>84–86</sup> Zhao and co-workers developed a dye-sensitized  $\text{TiO}_2$  composite incorporating alizarin red as the visible light absorbing dye and the nitrosyl radical TEMPO.<sup>87</sup> The combination of dye sensitized  $\text{TiO}_2$  and TEMPO produced an efficient photocatalytic system for selective oxidation of alcohol under visible light irradiation at ambient condition. Visible light irradiation of the dye anchored on  $\text{TiO}_2$  surface produces excited dye molecules, which in turn injects electrons to the conduction band of  $\text{TiO}_2$  and generates dye radical cation. The dye radical cation can in turn oxidize TEMPO to regenerate the dye and TEMPO<sup>•</sup>. The oxidized TEMPO<sup>•</sup> can further oxidize various alcohols to the corresponding aldehydes and regenerates the nitroxyl radical TEMPO.<sup>87</sup> The sensitization principle also finds important applications in the development of dye-sensitized solar cells (DSSC), which are third generation photovoltaics based on nanocrystalline large band gap semiconductors and highly efficient light harvesting molecular antennas.<sup>85</sup> In fact, metal-porphyrins<sup>7</sup> and Ru(II) polypyridyl<sup>9</sup> complexes have gained considerable attention in this context due to the presence of extensive delocalized  $\pi$ -electron system and strong absorption band in the visible region. Recently, Lin and co-workers have reported the development of a series of porphyrins for the application in DSSC containing anthracene in combination with pyrene or 4-dimethylaminophenyl group that show absorption in the NIR region.<sup>88,89</sup> The rapid electron injection and regeneration steps are crucial for the optimal activity of the system. Thus, the use of a porphyrin sensitizer (SM315) with the cobalt (II/III) redox couple led to the current 13% power conversion efficiency record.<sup>89</sup>

In a recent investigation, Chen et al. developed an alternative approach to enhance the visible light response of  $\text{TiO}_2$  by introducing disorders using hydrogenation in the surface layers of nanophase  $\text{TiO}_2$ , resulting in  $\text{TiO}_2$  particles absorbing in the visible and NIR wavelength region (Figure 8).<sup>90</sup> The unique photophysics of these “black  $\text{TiO}_2$ ” presumably results from the presence of energy states corresponding to the disorder above valence band as well as fast exchange of hydrogens.<sup>90</sup> It has also been suggested that hydrogenation of  $\text{TiO}_2$  nanowires

generates a high degree of oxygen vacancies that act as electron donor states lying about 0.75 and 1.18 eV below the conduction band of hydrogenated rutile  $\text{TiO}_2$ .<sup>91</sup> The visible and NIR absorption of “black  $\text{TiO}_2$ ” can be assigned to the transitions from  $\text{TiO}_2$  valence band to the oxygen vacancy levels or from the oxygen vacancy states to the  $\text{TiO}_2$  conduction band (as shown in Figure 8B).

Core-shell structured “black  $\text{TiO}_2$ ” nanoparticles with a rutile core and sulfide shell have been developed that showed significantly enhanced photocatalytic activity and efficient photochemical water splitting compared to pristine rutile  $\text{TiO}_2$ .<sup>92</sup> Synthesis of such “black  $\text{TiO}_2$ ” through reduction of  $\text{TiO}_2$  using molten aluminum creates a disordered surface layer with a large amount of  $\text{Ti}^{3+}$  and oxygen vacancies. These defects create localized energy states in the band gap and account for the visible and NIR light activity of these nanoparticles. Furthermore, the  $\text{S}^{2-}$  ions from the outer sulfide shell can occupy the oxygen vacancy sites and contributes to the further narrowing of the band gap.

In an attempt to enhance the visible and infrared light activity, gray  $\text{TiO}_2$  consisting of a  $\text{TiO}_{2-x}$  (core)/ $\text{TiO}_2$  (shell) nanowires using metallic aluminum as the reducing agent has also been synthesized.<sup>93</sup> These nanowires of  $\text{TiO}_2$  showed significantly higher solar-light driven photocatalytic efficiency than the standard Degussa (Evonik) P25. The activity under dark and visible light irradiated conditions enhanced strongly with an increase in reaction temperature. Photoluminescence studies revealed that annealing of  $\text{TiO}_2$  at elevated temperatures under reducing atmosphere generates oxygen vacancies, which act as electron traps and lower the recombination of photoinduced electrons and holes and result in a quenching of luminescence intensity.

Important developments have recently been made in the field of perovskite materials ( $\text{X}^{\text{II}}\text{A}^{2+\text{VI}}\text{B}^{4+\text{X}^{2-}}_3$ ), a class of compounds that have the same type of crystal structure as calcium titanate ( $\text{CaTiO}_3$ ).<sup>94–96</sup> In recent years, several perovskite related materials have been developed that showed enhanced visible light driven  $\text{H}_2$  production and decomposition of organic pollutants.<sup>96–98</sup> Both cationic and anionic dopants have been introduced into the layered perovskite-based metal oxide structure to tune the band gap positions required for visible-light-active photocatalysts.<sup>99–102</sup> The presence of anionic or cationic monodopants in perovskite-structure-based photo-



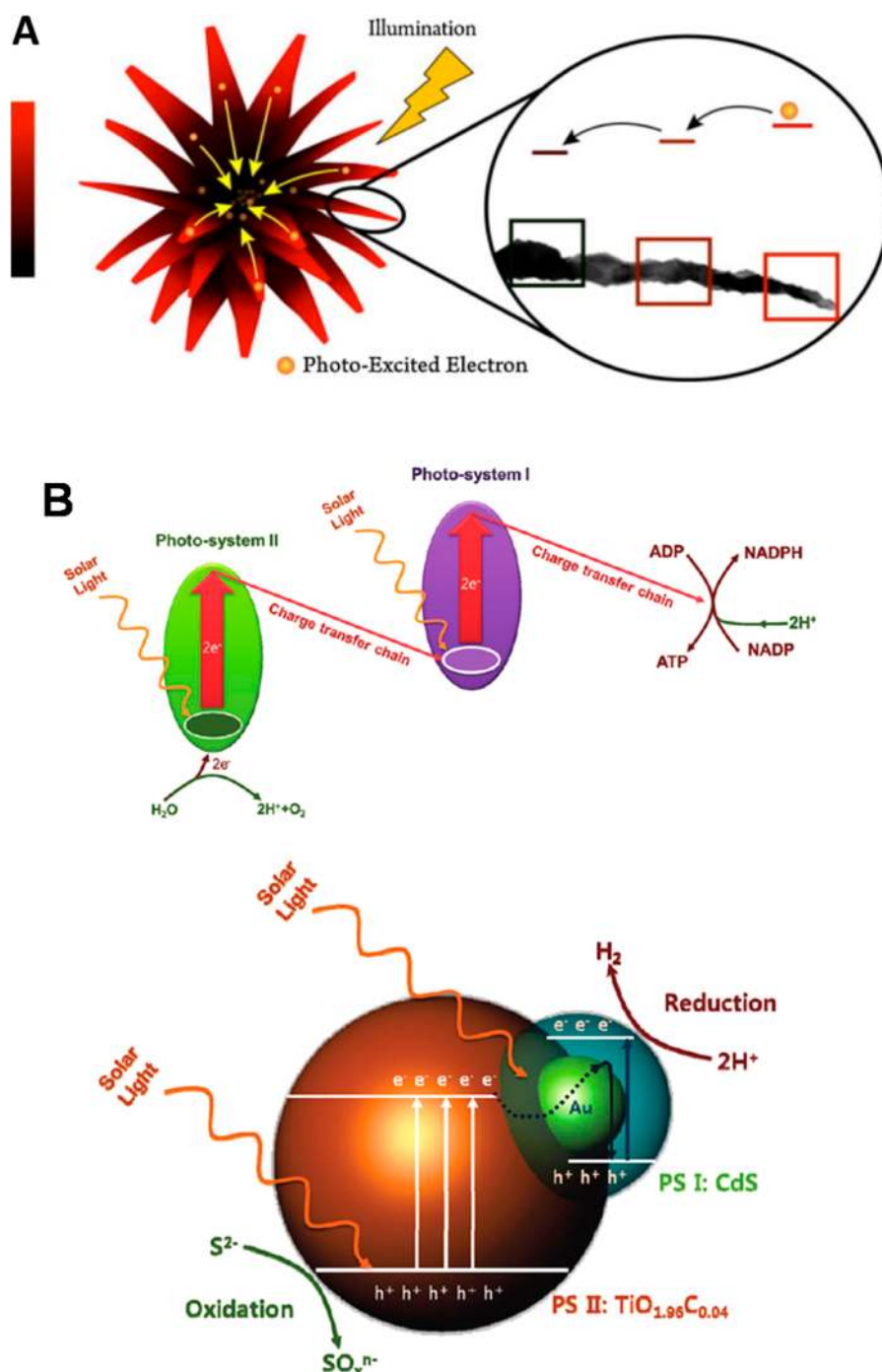


**Figure 9.** (A) The schematic illustration showing cascade of electron transfer in a nano/macro hierarchically structured TiO<sub>2</sub> upon illumination (ref 105). Copyright 2013, reprinted with permission from Elsevier. (B) Proposed Z-scheme mechanisms of the photosynthesis system: in natural photosynthesis system (top) and artificial CdS/Au/TiO<sub>1.96</sub>C<sub>0.04</sub> photosynthesis system (bottom) (ref 107). Copyright 2011, reprinted with permission from American Chemical Society.

catalysts such as Sr<sub>2</sub>Ta<sub>2</sub>O<sub>7</sub> and La<sub>2</sub>Ti<sub>2</sub>O<sub>7</sub> creates additional impurity energy levels in the band gap and reduces the effective band gap.<sup>100,101</sup> However, these energy states also act as electron–hole recombination centers and decreases the photocatalytic efficiency, which can be overcome by systemically designing cationic–anionic codoped systems.<sup>100,101</sup> Chen and co-workers reported the synthesis of Cr-doped SrTi<sub>1-x</sub>Cr<sub>x</sub>O<sub>3</sub> and Bi<sub>4</sub>Ti<sub>3-x</sub>Cr<sub>x</sub>O<sub>12</sub> that showed enhanced photocatalytic H<sub>2</sub> production activity under visible light illumination ( $\lambda > 420$  nm). DFT calculations suggested that doping with Cr generates

Cr 3d energy states in the band gap and the visible light absorption arises from the charge transfer from Cr 3d orbitals to Cr 3d + Ti 3d hybrid upon photoexcitation of the doped material.<sup>102</sup> Very recently, perovskite solar cells have emerged as cost-effective, high-efficiency systems for solar energy conversion to electricity. In fact, photovoltaic devices based on organic–inorganic [e.g., CH<sub>3</sub>NH<sub>3</sub>PbI<sub>3</sub>]<sup>94–96</sup> or inorganic [e.g., p-type CsSnI<sub>3</sub>]<sup>94</sup> perovskite structured semiconductors achieved power conversion efficiencies higher than 16% and were included in the “Science’s Top 10 Breakthroughs of

2013".<sup>94</sup> Moreover, current research on perovskites solar cells has proved the possibility of fine-tuning the optoelectronic properties (including energy gap and charge mobility) of materials, leading to increased light absorption, low charge recombination, and lasing ability,<sup>103</sup> properties that could be further optimized and exploited in the field of VLA photocatalysis.

There has been an exponential growth in research on development of visible-light-active TiO<sub>2</sub> photocatalysis over the last few decades after the discovery of VLA of N-doped TiO<sub>2</sub>. The field of solar light driven photocatalysis of TiO<sub>2</sub> is still expanding due to its wide range of applications in various fields including photoelectrochemical water splitting, reduction of CO<sub>2</sub>, and environmental remediation. In addition to dye sensitization, doping with metals and nonmetals, formation of heterojunctions have been widely used to enhance the visible light response of TiO<sub>2</sub> materials. Recently, perovskite-based layered metal oxides have also received tremendous attention for their applications in photoinduced processes, including their use in solar cells and as photocatalytic materials for removal of environmental pollutants. In recent years, quantum dots are appearing as excellent candidates for sensitization of TiO<sub>2</sub> for applications in photocatalysis and photovoltaics because of their interesting photophysical properties (high extinction coefficient, and quantum yield of emission), ease of synthesis, and the possibility to tune band gap.<sup>104</sup> However, a key factor in obtaining high efficiency of the photoconversion process is to facilitate the migration and separation of the charge carriers and increase the lifetime of the charge-separated species. Therefore, it is of critical importance to understand the excited state dynamics of the semiconductor material upon photoexcitation, which can shed light on the mechanistic aspects of the process as well as proves crucial in developing new materials with enhanced process efficiency. The importance of structural hierarchy in promoting charge migration and separation has been recently elucidated using chrysanthemum-like (ornamental-flower-like structure) TiO<sub>2</sub> structures with leafy branches.<sup>105</sup> The grain sizes in the branches increase gradually from nanoscale to microscale range along the direction of tip of the branches toward the center. The gradual size variation resulted in a series of heterojunctions between grains of different sizes, where the energy decreases gradually with increasing grain size. Thus, irradiation of this structure results excitation of electrons at the tip followed by a cascade of electron transfer as demonstrated in Figure 9A toward the central matrix leading to an efficient separation of charge carriers and improved photocatalytic properties.

To replicate the structural hierarchy and light harvesting ability of green leaves, *morph*-structured TiO<sub>2</sub> composites have been synthesized based on green leaves as templates.<sup>106</sup> Green leaves were initially treated with acid followed by TiCl<sub>3</sub> solution to substitute the Mg<sup>2+</sup> in chloroplast by Ti<sup>3+</sup> ions to generate the Ti-substituted layered nanostructure of thylakoid membrane. This was followed by reaction with Ti(OBu)<sub>4</sub> to generate the porous TiO<sub>2</sub> network replicating the vascular structure of green leaves. The *morph* structured TiO<sub>2</sub> derived from green leaf templates were doped with nitrogen from green leaves, and the N content was shown to depend on the leaf source. The high photocatalytic activity exhibited by the *morph*-TiO<sub>2</sub> composites has been assigned to the higher light harvesting ability of the porous and layered nanostructure and enhanced visible light absorption due to doping of nitrogen atoms from green leaves.

Several research groups have developed heterojunction structures derived from TiO<sub>2</sub> to promote directional electron transfer and facilitate charge separation to mimic the so-called Z-scheme of electron transport occurring in green leaves during photosynthesis.<sup>107,108</sup> Yun et al. reported the synthesis of carbon-doped titania (TiO<sub>2-x</sub>C<sub>x</sub>) acting as photosystem II (PSII) combined with a Au/CdS core-shell structure, functioning as photosystem I (PSI).<sup>107</sup> Upon visible light irradiation, the photoexcited electrons from the conduction band of TiO<sub>2-x</sub>C<sub>x</sub> move to CdS (PSI) through the Au core and combine with the photogenerated holes at the valence band of CdS (Figure 9B). These vectorial electron transports consequently increase the lifetime of conduction band electrons at the CdS (PSI) site, which can efficiently generate H<sub>2</sub> via the photocatalytic reduction of H<sub>2</sub>O. Tada and co-workers reported development of a similar nanoheterojunction consisting of CdS(PSI)/Au/TiO<sub>2</sub>(PSII) that exhibited very high activity for photocatalytic reduction of methyl viologen.<sup>108</sup> The enhanced photocatalytic activity has been attributed to the simultaneous excitation of both CdS and TiO<sub>2</sub> centers and vectorial electron transfer from the conduction band of TiO<sub>2</sub> to CdS via Au core.

The results obtained to date strongly indicate the critical necessity for further development of these groups of photocatalytic materials driven by solar light by combining the visible light activity with structural modification to achieve long-lived charge carriers, for applications in energy conversion, and environmental remediation purposes.

The results obtained to date strongly indicate the critical necessity for further development of these groups of photocatalytic materials driven by solar light by combining the visible light activity with structural modification to achieve long-lived charge carriers, for applications in energy conversion, and environmental remediation purposes. Important developments in the field are also expected for the use of VLA materials in tandem PEC-DSC cells for self-driven solar water splitting and CO<sub>2</sub> photocatalytic conversion (reduction path) to hydrocarbons.

## ■ AUTHOR INFORMATION

### Corresponding Authors

\*E-mail: pillai.suresh@itsligo.ie

\*E-mail: dionysdd@ucmail.uc.edu.

### Notes

The authors declare no competing financial interest.

### Biographies

Swagata Banerjee completed her B.Sc. from Presidency College and M.Sc. from the University of Calcutta, India. She obtained her Ph.D. degree (2012) under the joint supervision of Prof. T. Gunnlaugsson and Prof. J. M. Kelly, Trinity College Dublin. She joined CREST-DIT in 2013, where her research involved developing titania-based photocatalysis.

**Suresh C. Pillai** obtained his Ph.D. from Trinity College Dublin, Ireland, and then performed a postdoctoral research at California Institute of Technology (Caltech), U. S. A. He has worked at CREST in DIT as a senior R&D manager before moving to Institute of Technology Sligo as a senior lecturer in nanotechnology. <http://www.pemcentre.ie/>.

**Polycarpus Falaras** (Research Director at NCSR "Demokritos"/Athens/Greece) studied Physics (1978–1982/Thessaloniki University/Greece) and received his DEA in Electrochemistry (1983) and Ph.D. in Chemistry (1986) from Paris VI University (France). He works on nanotechnology-driven photoinduced processes and their application to solar energy conversion and environmental protection. <http://ipc.chem.demokritos.gr/>.

**Kevin O'Shea** earned B.S. degree with honors from CSU, Sacramento, and Ph.D. from UCLA in Chemistry. He is currently Professor of Chemistry and Senior Associate Dean of the Graduate School at Florida International University. His primary research interests are the reactions of reactive oxygen species (ROS) with organic compounds. <http://www2.fiu.edu/~osheak/index.html>.

**J. Anthony Byrne** is a Professor of Photocatalysis in the Nanotechnology and Integrated BioEngineering Centre at the University of Ulster. His main research interests lie in the fabrication, characterisation, and application of photocatalytic materials. Applications of interest include the photocatalytic treatment of water, the decontamination of surfaces, solar water splitting, and CO<sub>2</sub> reduction. <http://www.nibec.ulster.ac.uk/staff/j.byrne>.

**Dionysios (Dion) D. Dionysiou** is currently a Professor of Environmental Engineering and Science Program at the University of Cincinnati. He teaches courses and performs research in the areas of water quality, treatment, and monitoring. He is the author or coauthor of over 200 refereed journal publications and his work has received over 6,000 citations with an H factor of 47. [http://ceas.uc.edu/bcee/Dr\\_Dionysios\\_Dionysiou.html](http://ceas.uc.edu/bcee/Dr_Dionysios_Dionysiou.html).

## ACKNOWLEDGMENTS

S.C.P., D.D.D., J.A.B., and K.O. wish to acknowledge financial support under the U. S.–Ireland R&D Partnership Initiative from the Science Foundation Ireland (SFI-grant number 10/US/11822(T)), Department of Employment and Learning Northern Ireland (DELNI), and the U. S. National Science Foundation-CBET (Award 1033317).

## REFERENCES

- (1) Pelaez, M.; Nolan, N. T.; Pillai, S. C.; Seery, M. K.; Falaras, P.; Kontos, A. G.; Dunlop, P. S. M.; Hamilton, J. W. J.; Byrne, J. A.; O'Shea, K.; et al. A Review on the Visible Light Active Titanium Dioxide Photocatalysts for Environmental Applications. *Appl. Catal., B* **2012**, *125*, 331–349.
- (2) Keane, D. A.; McGuigan, K. G.; Ibanez, P. F.; Polo-Lopez, M. I.; Byrne, J. A.; Dunlop, P. S. M.; O'Shea, K.; Dionysiou, D. D.; Pillai, S. C. Solar Photocatalysis for Water Disinfection: Materials and Reactor Design. *Catal. Sci. Technol.* **2014**, *4*, 1211–1226.
- (3) Qu, Y.; Duan, X. Progress, Challenge and Perspective of Heterogeneous Photocatalysts. *Chem. Soc. Rev.* **2013**, *42*, 2568–2580.
- (4) Fisher, M. B.; Keane, D. A.; Fernández-Ibáñez, P.; Colreavy, J.; Hinder, S. J.; McGuigan, K. G.; Pillai, S. C. Nitrogen and Copper Doped Solar Light Active TiO<sub>2</sub> Photocatalysts for Water Decontamination. *Appl. Catal., B* **2013**, *130–131*, 8–13.
- (5) Fujishima, A.; Honda, K. Electrochemical Photolysis of Water at a Semiconductor Electrode. *Nature* **1972**, *238*, 37–38.
- (6) Li, X.; Liu, L.; Kang, S.-Z.; Mu, J.; Li, G. Differences Between Zn-Porphyrin-Coupled Titanate Nanotubes with Various Anchoring

Modes: Thermostability, Spectroscopic, Photocatalytic and Photo-electronic Properties. *Appl. Surf. Sci.* **2011**, *257*, 5950–5956.

(7) Afzal, S.; Daoud, W. A.; Langford, S. J. Photostable Self-Cleaning Cotton by a Copper(II) Porphyrin/TiO<sub>2</sub> Visible-Light Photocatalytic System. *ACS Appl. Mater. Interfaces* **2013**, *5*, 4753–4759.

(8) Wu, S.-H.; Wu, J.-L.; Jia, S.-Y.; Chang, Q.-W.; Ren, H.-T.; Liu, Y. Cobalt(II) Phthalocyanine-Sensitized Hollow Fe<sub>3</sub>O<sub>4</sub>@SiO<sub>2</sub>@TiO<sub>2</sub> Hierarchical Nanostructures: Fabrication and Enhanced Photocatalytic Properties. *Appl. Surf. Sci.* **2013**, *287*, 389–396.

(9) Cho, Y.; Choi, W.; Lee, C.-H.; Hyeon, T.; Lee, H.-I. Visible Light-Induced Degradation of Carbon Tetrachloride on Dye-Sensitized TiO<sub>2</sub>. *Environ. Sci. Technol.* **2001**, *35*, 966–970.

(10) Qi, B.; Yu, Y.; He, X.; Wu, L.; Duan, X.; Zhi, J. Series of Transition Metal-Doped TiO<sub>2</sub> Transparent Aqueous Sols with Visible-Light Response. *Mater. Chem. Phys.* **2012**, *135*, 549–553.

(11) Serpone, N.; Lawless, D.; Disdier, J.; Herrmann, J.-M. Spectroscopic, Photoconductivity, and Photocatalytic Studies of TiO<sub>2</sub> Colloids: Naked and with the Lattice Doped with Cr<sup>3+</sup>, Fe<sup>3+</sup>, and V<sup>5+</sup> Cations. *Langmuir* **1994**, *10*, 643–652.

(12) Inturi, S. N. R.; Boningari, T.; Suidan, M.; Smirniotis, P. G. Visible-Light-Induced Photodegradation of Gas Phase Acetonitrile Using Aerosol-Made Transition Metal (V, Cr, Fe, Co, Mn, Mo, Ni, Cu, Y, Ce, and Zr) Doped TiO<sub>2</sub>. *Appl. Catal., B* **2014**, *144*, 333–342.

(13) Xu, J.; Ao, Y.; Fu, D.; Yuan, C. A Simple Route for the Preparation of Eu, N-Codoped TiO<sub>2</sub> Nanoparticles with Enhanced Visible Light-Induced Photocatalytic Activity. *J. Colloid Interface Sci.* **2008**, *328*, 447–451.

(14) Devi, L. G.; Kumar, S. G. Exploring the Critical Dependence of Adsorption of Various Dyes on the Degradation Rate Using Ln<sup>3+</sup>-TiO<sub>2</sub> Surface under UV/Solar Light. *Appl. Surf. Sci.* **2012**, *261*, 137–146.

(15) Han, C.; Pelaez, M.; Likodimos, V.; Kontos, A. G.; Falaras, P.; O'Shea, K.; Dionysiou, D. D. Innovative Visible Light-Activated Sulfur Doped TiO<sub>2</sub> Films for Water Treatment. *Appl. Catal., B* **2011**, *107*, 77–87.

(16) Periyat, P.; Pillai, S. C.; McCormack, D. E.; Colreavy, J.; Hinder, S. J. Improved High-Temperature Stability and Sun-Light-Driven Photocatalytic Activity of Sulfur-Doped Anatase TiO<sub>2</sub>. *J. Phys. Chem. C* **2008**, *112*, 7644–7652.

(17) Dozzi, M. V.; Selli, E. Doping TiO<sub>2</sub> with *p*-Block Elements: Effects on Photocatalytic Activity. *J. Photochem. Photobiol. C* **2013**, *14*, 13–28.

(18) Khan, S. U. M.; Al-Shahry, M.; Ingler, W. B. Efficient Photochemical Water Splitting by a Chemically Modified n-TiO<sub>2</sub>. *Science* **2002**, *297*, 2243–2245.

(19) Mohapatra, S. K.; Misra, M.; Mahajan, V. K.; Raja, K. S. Design of a Highly Efficient Photoelectrolytic Cell for Hydrogen Generation by Water Splitting: Application of TiO<sub>2-x</sub>C<sub>x</sub> Nanotubes as a Photoanode and Pt/TiO<sub>2</sub> Nanotubes as a Cathode. *J. Phys. Chem. C* **2007**, *111*, 8677–8685.

(20) Sakthivel, S.; Kisch, H. Daylight Photocatalysis by Carbon-Modified Titanium Dioxide. *Angew. Chem., Int. Ed.* **2003**, *42*, 4908–4911.

(21) Dong, F.; Guo, S.; Wang, H.; Li, X.; Wu, Z. Enhancement of the Visible Light Photocatalytic Activity of C-Doped TiO<sub>2</sub> Nanomaterials Prepared by a Green Synthetic Approach. *J. Phys. Chem. C* **2011**, *115*, 13285–13292.

(22) Irie, H.; Watanabe, Y.; Hashimoto, K. Carbon-Doped Anatase TiO<sub>2</sub> Powders as a Visible-Light Sensitive Photocatalyst. *Chem. Lett.* **2003**, *32*, 772–773.

(23) Huang, Y.; Ho, W.; Lee, S.; Zhang, L.; Li, G.; Yu, J. C. Effect of Carbon Doping on the Mesoporous Structure of Nanocrystalline Titanium Dioxide and Its Solar-Light-Driven Photocatalytic Degradation of NO<sub>x</sub>. *Langmuir* **2008**, *24*, 3510–3516.

(24) Gole, J. L.; Stout, J. D.; Burda, C.; Lou, Y.; Chen, X. Highly Efficient Formation of Visible Light Tunable TiO<sub>2-x</sub>N<sub>x</sub> Photocatalysts and Their Transformation at the Nanoscale. *J. Phys. Chem. B* **2003**, *108*, 1230–1240.

- (25) Pelaez, M.; Baruwati, B.; Varma, R. S.; Luque, R.; Dionysiou, D. D. Microcystin-LR Removal from Aqueous Solutions Using a Magnetically Separable N-Doped TiO<sub>2</sub> Nanocomposite under Visible Light Irradiation. *Chem. Commun.* **2013**, *49*, 10118–10120.
- (26) Nolan, N. T.; Synnott, D. W.; Seery, M. K.; Hinder, S. J.; Van Wassenhoven, A.; Pillai, S. C. Effect of N-Doping on the Photocatalytic Activity of Sol-Gel TiO<sub>2</sub>. *J. Hazard. Mater.* **2012**, *211*, 88–94.
- (27) Umabayashi, T.; Yamaki, T.; Tanaka, S.; Asai, K. Visible Light-Induced Degradation of Methylene Blue on S-doped TiO<sub>2</sub>. *Chem. Lett.* **2003**, *32*, 330–331.
- (28) Ohno, T.; Akiyoshi, M.; Umabayashi, T.; Asai, K.; Mitsui, T.; Matsumura, M. Preparation of S-Doped TiO<sub>2</sub> Photocatalysts and Their Photocatalytic Activities under Visible Light. *Appl. Catal., A* **2004**, *265*, 115–121.
- (29) Umabayashi, T.; Yamaki, T.; Tanaka, S.; Asai, K. Visible Light-Induced Degradation of Methylene Blue on S-doped TiO<sub>2</sub>. *Chem. Lett.* **2003**, *32*, 330–331.
- (30) Sato, S. Photocatalytic Activity of NO<sub>x</sub>-Doped TiO<sub>2</sub> in the Visible Light Region. *Chem. Phys. Lett.* **1986**, *123*, 126–128.
- (31) Asahi, R.; Morikawa, T.; Ohwaki, T.; Aoki, K.; Taga, Y. Visible-Light Photocatalysis in Nitrogen-Doped Titanium Oxides. *Science* **2001**, *293*, 269–271.
- (32) Serpone, N. Is the Band Gap of Pristine TiO<sub>2</sub> Narrowed by Anion- and Cation-Doping of Titanium Dioxide in Second-Generation Photocatalysts? *J. Phys. Chem. B* **2006**, *110*, 24287–24293.
- (33) Di Valentin, C.; Pacchioni, G. Trends in Non-Metal Doping of Anatase TiO<sub>2</sub>: B, C, N and F. *Catal. Today* **2013**, *206*, 12–18.
- (34) Napoli, F.; Chiesa, M.; Livraghi, S.; Giamello, E.; Agnoli, S.; Granozzi, G.; Pacchioni, G.; Di Valentin, C. The Nitrogen Photoactive Centre in N-Doped Titanium Dioxide Formed via Interaction of N Atoms with the Solid. Nature and Energy Level of the Species. *Chem. Phys. Lett.* **2009**, *477*, 135–138.
- (35) Di Valentin, C.; Pacchioni, G.; Selloni, A.; Livraghi, S.; Giamello, E. Characterization of Paramagnetic Species in N-Doped TiO<sub>2</sub> Powders by EPR Spectroscopy and DFT Calculations. *J. Phys. Chem. B* **2005**, *109*, 11414–11419.
- (36) Di Valentin, C.; Finazzi, E.; Pacchioni, G.; Selloni, A.; Livraghi, S.; Paganini, M. C.; Giamello, E. N-doped TiO<sub>2</sub>: Theory and Experiment. *Chem. Phys.* **2007**, *339*, 44–56.
- (37) Etacheri, V.; Seery, M. K.; Hinder, S. J.; Pillai, S. C. Oxygen Rich Titania: A Dopant Free, High Temperature Stable, and Visible-Light Active Anatase Photocatalyst. *Adv. Funct. Mater.* **2011**, *21*, 3744–3752.
- (38) Xu, J.-H.; Li, J.; Dai, W.-L.; Cao, Y.; Li, H.; Fan, K. Simple Fabrication of Twist-Like Helix N,S-Codoped Titania Photocatalyst with Visible-Light Response. *Appl. Catal., B* **2008**, *79*, 72–80.
- (39) Liu, G.; Zhao, Y.; Sun, C.; Li, F.; Lu, G. Q.; Cheng, H.-M. Synergistic Effects of B/N Doping on the Visible-Light Photocatalytic Activity of Mesoporous TiO<sub>2</sub>. *Angew. Chem., Int. Ed.* **2008**, *47*, 4516–4520.
- (40) Liu, G.; Han, C.; Pelaez, M.; Zhu, D.; Liao, S.; Likodimos, V.; Kontos, A. G.; Falaras, P.; Dionysiou, D. D. Enhanced Visible Light Photocatalytic Activity of C-N-Codoped TiO<sub>2</sub> Films for the Degradation of Microcystin-LR. *J. Mol. Catal. A: Chem.* **2013**, *372*, 58–65.
- (41) Periyat, P.; McCormack, D. E.; Hinder, S. J.; Pillai, S. C. One-Pot Synthesis of Anionic (Nitrogen) and Cationic (Sulfur) Codoped High-Temperature Stable, Visible Light Active, Anatase Photocatalysts. *J. Phys. Chem. C* **2009**, *113*, 3246–3253.
- (42) Katsanaki, A. V.; Kontos, A. G.; Maggos, T.; Pelaez, M.; Likodimos, V.; Pavlatou, E. A.; Dionysiou, D. D.; Falaras, P. Photocatalytic Oxidation of Nitrogen Oxides on N-F-Doped Titania Thin Films. *Appl. Catal., B* **2013**, *140*, 619–625.
- (43) Pelaez, M.; Falaras, P.; Kontos, A. G.; de la Cruz, A. A.; O'Shea, K.; Dunlop, P. S. M.; Byrne, J. A.; Dionysiou, D. D. A Comparative Study on the Removal of Cytochrome P-450 and Microcystins from Water with NF-TiO<sub>2</sub>-P25 Composite Films with Visible and UV-Vis Light Photocatalytic Activity. *Appl. Catal., B* **2012**, *121*, 30–39.
- (44) Kontos, A. G.; Pelaez, M.; Likodimos, V.; Vaenas, N.; Dionysiou, D. D.; Falaras, P. Visible Light Induced Wetting of Nanostructured N-F Co-Doped Titania Films. *Photochem. Photobiol. Sci.* **2011**, *10*, 350–354.
- (45) Pelaez, M.; Falaras, P.; Likodimos, V.; Kontos, A. G.; de la Cruz, A. A.; O'Shea, K.; Dionysiou, D. D. Synthesis, Structural Characterization and Evaluation of Sol-Gel-Based NF-TiO<sub>2</sub> Films with Visible Light-Photoactivation for the Removal of Microcystin-LR. *Appl. Catal., B* **2010**, *99*, 378–387.
- (46) Pelaez, M.; de la Cruz, A. A.; Stathatos, E.; Falaras, P.; Dionysiou, D. D. Visible Light-Activated N-F-Codoped TiO<sub>2</sub> Nanoparticles for the Photocatalytic Degradation of Microcystin-LR in Water. *Catal. Today* **2009**, *144*, 19–25.
- (47) Zhao, C.; Pelaez, M.; Dionysiou, D. D.; Pillai, S. C.; Byrne, J. A.; O'Shea, K. E. UV and Visible Light Activated TiO<sub>2</sub> Photocatalysis of 6-Hydroxymethyl Uracil, a Model Compound for the Potent Cyanotoxin Cytochrome P-450. *Catal. Today* **2014**, *224*, 70–76.
- (48) Hamilton, J. W. J.; Byrne, J. A.; Dunlop, P. S. M.; Dionysiou, D. D.; Pelaez, M.; O'Shea, K.; Synnott, D.; Pillai, S. C. Evaluating the Mechanism of Visible Light Activity for N,F-TiO<sub>2</sub> Using Photoelectrochemistry. *J. Phys. Chem. C* **2014**, *118*, 12206–12215.
- (49) Rengifo-Herrera, J. A.; Pulgarin, C. Photocatalytic Activity of N, S Co-Doped and N-Doped Commercial Anatase TiO<sub>2</sub> Powders Towards Phenol Oxidation and *E. coli* Inactivation under Simulated Solar Light Irradiation. *Sol. Energy* **2010**, *84*, 37–43.
- (50) Rengifo-Herrera, J. A.; Pierzchała, K.; Sienkiewicz, A.; Forró, L.; Kiwi, J.; Pulgarin, C. Abatement of Organics and *Escherichia coli* by N, S Co-Doped TiO<sub>2</sub> under UV and Visible Light. Implications of the Formation of Singlet Oxygen (<sup>1</sup>O<sub>2</sub>) under Visible Light. *Appl. Catal., B* **2009**, *88*, 398–406.
- (51) Ma, X.; Dai, Y.; Guo, M.; Huang, B. Insights into the Role of Surface Distortion in Promoting the Separation and Transfer of Photogenerated Carriers in Anatase TiO<sub>2</sub>. *J. Phys. Chem. C* **2013**, *117*, 24496–24502.
- (52) Moustakas, N. G.; Kontos, A. G.; Likodimos, V.; Katsaros, F.; Boukos, N.; Tsoutsou, D.; Dimoulas, A.; Romanos, G. E.; Dionysiou, D. D.; Falaras, P. Inorganic–Organic Core–Shell Titania Nanoparticles for Efficient Visible Light Activated Photocatalysis. *Appl. Catal., B* **2013**, *130–131*, 14–24.
- (53) Di Paola, A.; García-López, E.; Ikeda, S.; Marci, G.; Ohtani, B.; Palmisano, L. Photocatalytic Degradation of Organic Compounds in Aqueous Systems by Transition Metal Doped Polycrystalline TiO<sub>2</sub>. *Catal. Today* **2002**, *75*, 87–93.
- (54) Seery, M. K.; George, R.; Floris, P.; Pillai, S. C. Silver Doped Titanium Dioxide Nanomaterials for Enhanced Visible Light Photocatalysis. *J. Photochem. Photobiol., A* **2007**, *189*, 258–263.
- (55) Cao, J.; Xu, B.; Luo, B.; Lin, H.; Chen, S. Preparation, Characterization and Visible-Light Photocatalytic Activity of Ag/AgCl/TiO<sub>2</sub>. *Appl. Surf. Sci.* **2011**, *257*, 7083–7089.
- (56) Arabatzis, I. M.; Stergiopoulos, T.; Bernard, M. C.; Labou, D.; Neophytides, S. G.; Falaras, P. Silver-Modified Titanium Dioxide Thin Films for Efficient Photodegradation of Methyl Orange. *Appl. Catal., B* **2003**, *42*, 187–201.
- (57) Nolan, N. T.; Seery, M. K.; Hinder, S. J.; Healy, L. F.; Pillai, S. C. A Systematic Study of the Effect of Silver on the Chelation of Formic Acid to a Titanium Precursor and the Resulting Effect on the Anatase to Rutile Transformation of TiO<sub>2</sub>. *J. Phys. Chem. C* **2010**, *114*, 13026–13034.
- (58) Kitano, S.; Murakami, N.; Ohno, T.; Mitani, Y.; Nosaka, Y.; Asakura, H.; Teramura, K.; Tanaka, T.; Tada, H.; Hashimoto, K.; Kominami, H. Bifunctionality of Rh<sup>3+</sup> Modifier on TiO<sub>2</sub> and Working Mechanism of Rh<sup>3+</sup>/TiO<sub>2</sub> Photocatalyst under Irradiation of Visible Light. *J. Phys. Chem. C* **2013**, *117*, 11008–11016.
- (59) Lincic, S.; Christopher, P.; Ingram, D. B. Plasmonic-Metal Nanostructures for Efficient Conversion of Solar to Chemical Energy. *Nat. Mater.* **2011**, *10*, 911–921.
- (60) Awazu, K.; Fujimaki, M.; Rockstuhl, C.; Tominaga, J.; Murakami, H.; Ohki, Y.; Yoshida, N.; Watanabe, T. A Plasmonic Photocatalyst Consisting of Silver Nanoparticles Embedded in Titanium Dioxide. *J. Am. Chem. Soc.* **2008**, *130*, 1676–1680.

- (61) Jang, Y. H.; Jang, Y. J.; Kochuveedu, S. T.; Byun, M.; Lin, Z.; Kim, D. H. Plasmonic Dye-Sensitized Solar cells Incorporated with Au-TiO<sub>2</sub> Nanostructures with Tailored Configurations. *Nanoscale* **2014**, *6*, 1823–1832.
- (62) Chandrasekharan, N.; Kamat, P. V. Improving the Photoelectrochemical Performance of Nanostructured TiO<sub>2</sub> Films by Adsorption of Gold Nanoparticles. *J. Phys. Chem. B* **2000**, *104*, 10851–10857.
- (63) Dawson, A.; Kamat, P. V. Semiconductor–Metal Nanocomposites. Photoinduced Fusion and Photocatalysis of Gold-Capped TiO<sub>2</sub> (TiO<sub>2</sub>/Gold) Nanoparticles. *J. Phys. Chem. B* **2001**, *105*, 960–966.
- (64) Subramanian, V.; Wolf, E. E.; Kamat, P. V. Catalysis with TiO<sub>2</sub>/Gold Nanocomposites. Effect of Metal Particle Size on the Fermi Level Equilibration. *J. Am. Chem. Soc.* **2004**, *126*, 4943–4950.
- (65) Furube, A.; Du, L.; Hara, K.; Katoh, R.; Tachiya, M. Ultrafast Plasmon-Induced Electron Transfer from Gold Nanodots into TiO<sub>2</sub> Nanoparticles. *J. Am. Chem. Soc.* **2007**, *129*, 14852–14853.
- (66) Choi, H.; Chen, W. T.; Kamat, P. V. Know Thy Nano Neighbor. Plasmonic versus Electron Charging Effects of Metal Nanoparticles in Dye-Sensitized Solar Cells. *ACS Nano* **2012**, *6*, 4418–4427.
- (67) Shiraishi, Y.; Sakamoto, H.; Sugano, Y.; Ichikawa, S.; Hirai, T. Pt-Cu Bimetallic Alloy Nanoparticles Supported on Anatase TiO<sub>2</sub>: Highly Active Catalysts for Aerobic Oxidation Driven by Visible Light. *ACS Nano* **2013**, *7*, 9287–9297.
- (68) Pan, X.; Xu, Y.-J. Defect-Mediated Growth of Noble-Metal (Ag, Pt, and Pd) Nanoparticles on TiO<sub>2</sub> with Oxygen Vacancies for Photocatalytic Redox Reactions under Visible Light. *J. Phys. Chem. C* **2013**, *117*, 17996–18005.
- (69) Xiao, F.-X. Construction of Highly Ordered ZnO–TiO<sub>2</sub> Nanotube Arrays (ZnO/TNTs) Heterostructure for Photocatalytic Application. *ACS Appl. Mater. Interfaces* **2012**, *4*, 7055–7063.
- (70) Liu, B.; Khare, A.; Aydil, E. S. TiO<sub>2</sub>–B/Anatase Core–Shell Heterojunction Nanowires for Photocatalysis. *ACS Appl. Mater. Interfaces* **2011**, *3*, 4444–4450.
- (71) Etacheri, V.; Michlits, G.; Seery, M. K.; Hinder, S. J.; Pillai, S. C. A Highly Efficient TiO<sub>2-x</sub>C<sub>x</sub> Nano-heterojunction Photocatalyst for Visible Light Induced Antibacterial Applications. *ACS Appl. Mater. Interfaces* **2013**, *5*, 1663–1672.
- (72) Etacheri, V.; Seery, M. K.; Hinder, S. J.; Pillai, S. C. Highly Visible Light Active TiO<sub>2-x</sub>N<sub>x</sub> Heterojunction Photocatalysts. *Chem. Mater.* **2010**, *22*, 3843–3853.
- (73) Etacheri, V.; Seery, M. K.; Hinder, S. J.; Pillai, S. C. Nanostructured Ti<sub>1-x</sub>S<sub>x</sub>O<sub>2-y</sub>N<sub>y</sub> Heterojunctions for Efficient Visible-Light-Induced Photocatalysis. *Inorg. Chem.* **2012**, *51*, 7164–7173.
- (74) Wang, Y.; Liu, L.; Xu, L.; Meng, C.; Zhu, W. Ag/TiO<sub>2</sub> Nanofiber Heterostructures: Highly Enhanced Photocatalysts under Visible Light. *J. Appl. Phys.* **2013**, *113*, 174311.
- (75) Huang, Z.-F.; Zou, J.-J.; Pan, L.; Wang, S.; Zhang, X.; Wang, L. Synergetic Promotion on Photoactivity and Stability of W<sub>18</sub>O<sub>49</sub>/TiO<sub>2</sub> hybrid. *Appl. Catal., B* **2014**, *147*, 167–174.
- (76) Zhao, W.; Ma, W.; Chen, C.; Zhao, J.; Shuai, Z. Efficient Degradation of Toxic Organic Pollutants with Ni<sub>2</sub>O<sub>3</sub>/TiO<sub>2-x</sub>B<sub>x</sub> under Visible Irradiation. *J. Am. Chem. Soc.* **2004**, *126*, 4782–4783.
- (77) Qin, W.; Zhang, D.; Zhao, D.; Wang, L.; Zheng, K. Near-Infrared Photocatalysis Based on YF<sub>3</sub>: Yb<sup>3+</sup>, Tm<sup>3+</sup>/TiO<sub>2</sub> Core/Shell Nanoparticles. *Chem. Commun.* **2010**, *46*, 2304–2306.
- (78) Guo, X.; Di, W.; Chen, C.; Liu, C.; Wang, X.; Qin, W. Enhanced Near-Infrared Photocatalysis of NaYF<sub>4</sub>:Yb, Tm/CdS/TiO<sub>2</sub> Composites. *Dalton Trans.* **2014**, *43*, 1048–1054.
- (79) Pastrana-Martínez, L. M.; Morales-Torres, S.; Likodimos, V.; Figueiredo, J. L.; Faria, J. L.; Falaras, P.; Silva, A. M. T. Advanced Nanostructured Photocatalysts Based on Reduced Graphene Oxide–TiO<sub>2</sub> Composites for Degradation of Diphenhydramine Pharmaceutical and Methyl Orange Dye. *Appl. Catal., B* **2012**, *123–124*, 241–256.
- (80) Miranda, S. M.; Romanos, G. E.; Likodimos, V.; Marques, R. R. N.; Favvas, E. P.; Katsaros, F. K.; Stefanopoulos, K. L.; Vilar, V. J. P.; Faria, J. L.; Falaras, P.; Silva, A. M. T. Pore Structure, Interface Properties and Photocatalytic Efficiency of Hydration/Dehydration Derived TiO<sub>2</sub>/CNT Composites. *Appl. Catal., B* **2014**, *147*, 65–81.
- (81) Moustakas, N. G.; Katsaros, F. K.; Kontos, A. G.; Romanos, G. E.; Dionysiou, D. D.; Falaras, P. Visible Light Active TiO<sub>2</sub> Photocatalytic Filtration Membranes with Improved Permeability and Low Energy Consumption. *Catal. Today* **2014**, *224*, 56–69.
- (82) Likodimos, V.; Han, C.; Pelaez, M.; Kontos, A. G.; Liu, G.; Zhu, D.; Liao, S.; de la Cruz, A. A.; O’Shea, K.; Dunlop, P. S. M.; Byrne, J. A.; Dionysiou, D. D.; Falaras, P. Anion-Doped TiO<sub>2</sub> Nanocatalysts for Water Purification under Visible Light. *Ind. Eng. Chem. Res.* **2013**, *52*, 13957–13964.
- (83) Romanos, G. E.; Athanasekou, C. P.; Likodimos, V.; Aloupogiannis, P.; Falaras, P. Hybrid Ultrafiltration/Photocatalytic Membranes for Efficient Water Treatment. *Ind. Eng. Chem. Res.* **2013**, *52*, 13938–13947.
- (84) Tsoukleris, D. S.; Kontos, A. I.; Aloupogiannis, P.; Falaras, P. Photocatalytic Properties of Screen-Printed Titania. *Catal. Today* **2007**, *124*, 110–117.
- (85) Falaras, P. Synergetic Effect of Carboxylic Acid Functional Groups and Fractal Surface Characteristics for Efficient Dye Sensitization of Titanium Oxide. *Sol. Energy Mater. Sol. Cells* **1998**, *53*, 163–175.
- (86) Zhao, J.; Chen, C.; Ma, W. Photocatalytic Degradation of Organic Pollutants Under Visible Light Irradiation. *Top. Catal.* **2005**, *35*, 269–278.
- (87) Zhang, M.; Chen, C.; Ma, W.; Zhao, J. Visible-Light-Induced Aerobic Oxidation of Alcohols in a Coupled Photocatalytic System of Dye-Sensitized TiO<sub>2</sub> and TEMPO. *Angew. Chem., Int. Ed.* **2008**, *47*, 9730–9733.
- (88) Wu, C.-H.; Chen, M.-C.; Su, P.-C.; Kuo, H.-H.; Wang, C.-L.; Lu, C.-Y.; Tsai, C.-H.; Wu, C.-C.; Lin, C.-Y. Porphyrins for Efficient Dye-Sensitized Solar Cells Covering the Near-IR Region. *J. Mater. Chem. A* **2014**, *2*, 991–999.
- (89) Mathew, S.; Yella, A.; Gao, P.; Humphry-Baker, R.; Curchod, B. F. E.; Ashari-Astani, N.; Tavernelli, I.; Rothlisberger, U.; Nazeeruddin, M. K.; Gratzel, M. Dye-Sensitized Solar Cells with 13% Efficiency Achieved Through the Molecular Engineering of Porphyrin Sensitizers. *Nat. Chem.* **2014**, *6*, 242–247.
- (90) Chen, X.; Liu, L.; Yu, P. Y.; Mao, S. S. Increasing Solar Absorption for Photocatalysis with Black Hydrogenated Titanium Dioxide Nanocrystals. *Science* **2011**, *331*, 746–750.
- (91) Wang, G.; Wang, H.; Ling, Y.; Tang, Y.; Yang, X.; Fitzmorris, R. C.; Wang, C.; Zhang, J. Z.; Li, Y. Hydrogen-Treated TiO<sub>2</sub> Nanowire Arrays for Photoelectrochemical Water Splitting. *Nano Lett.* **2011**, *11*, 3026–3033.
- (92) Yang, C.; Wang, Z.; Lin, T.; Yin, H.; Lü, X.; Wan, D.; Xu, T.; Zheng, C.; Lin, J.; Huang, F.; Xie, X.; Jiang, M. Core-Shell Nanostructured “Black” Rutile Titania as Excellent Catalyst for Hydrogen Production Enhanced by Sulfur Doping. *J. Am. Chem. Soc.* **2013**, *135*, 17831–17838.
- (93) Yin, H.; Lin, T.; Yang, C.; Wang, Z.; Zhu, G.; Xu, T.; Xie, X.; Huang, F.; Jiang, M. Gray TiO<sub>2</sub> Nanowires Synthesized by Aluminum-Mediated Reduction and Their Excellent Photocatalytic Activity for Water Cleaning. *Chem.—Eur. J.* **2013**, *19*, 13313–13316.
- (94) Chung, I.; Lee, B.; He, J.; Chang, R. P. H.; Kanatzidis, M. G. All-Solid-State Dye-Sensitized Solar Cells with High Efficiency. *Nature* **2012**, *485*, 486–494.
- (95) Liu, M.; Johnston, M. B.; Snaith, H. J. Efficient Planar Heterojunction Perovskite Solar Cells by Vapour Deposition. *Nature* **2013**, *501*, 395–398.
- (96) Snaith, H. J. Perovskites: The Emergence of a New Era for Low-Cost, High-Efficiency Solar Cells. *J. Phys. Chem. Lett.* **2013**, *4*, 3623–3630.
- (97) Kako, T.; Zou, Z.; Ye, J. Photocatalytic Oxidation of 2-Propanol in the Gas Phase Over Cesium Bismuth Niobates under Visible Light Irradiation. *Res. Chem. Intermediat.* **2005**, *31*, 359–364.
- (98) Fu, Q.; Li, J. L.; He, T.; Yang, G. W. Band-Engineered CaTiO<sub>3</sub> Nanowires for Visible Light Photocatalysis. *J. Appl. Phys.* **2013**, *113*, 104303.

- (99) Mukherji, A.; Seger, B.; Lu, G. Q.; Wang, L. Nitrogen Doped  $\text{Sr}_2\text{Ta}_2\text{O}_7$  Coupled with Graphene Sheets as Photocatalysts for Increased Photocatalytic Hydrogen Production. *ACS Nano* **2011**, *5*, 3483–3492.
- (100) Liu, P.; Nisar, J.; Ahuja, R.; Pathak, B. Layered Perovskite  $\text{Sr}_2\text{Ta}_2\text{O}_7$  for Visible Light Photocatalysis: A First Principles Study. *J. Phys. Chem. C* **2013**, *117*, 5043–5050.
- (101) Liu, P.; Nisar, J.; Pathak, B.; Ahuja, R. Cationic-Anionic Mediated Charge Compensation on  $\text{La}_2\text{Ti}_2\text{O}_7$  for Visible Light Photocatalysis. *Phys. Chem. Chem. Phys.* **2013**, *15*, 17150–17157.
- (102) Liu, J. W.; Chen, G.; Li, Z. H.; Zhang, Z. G. Electronic Structure and Visible Light Photocatalysis Water Splitting Property of Chromium-Doped  $\text{SrTiO}_3$ . *J. Solid State Chem.* **2006**, *179*, 3704–3708.
- (103) Deschler, F.; Price, M.; Pathak, S.; Klintberg, L. E.; Jarausch, D.-D.; Higler, R.; Hüttner, S.; Leijtens, T.; Stranks, S. D.; Snaith, H. J.; Atatüre, M.; Phillips, R. T.; Friend, R. H. High Photoluminescence Efficiency and Optically Pumped Lasing in Solution-Processed Mixed Halide Perovskite Semiconductors. *J. Phys. Chem. Lett.* **2014**, *5*, 1421–1426.
- (104) Kamat, P. V. Quantum Dot Solar Cells. The Next Big Thing in Photovoltaics. *J. Phys. Chem. Lett.* **2013**, *4*, 908–918.
- (105) Chen, P.-C.; Tsai, M.-C.; Yang, M.-H.; Chen, T.-T.; Chen, H.-C.; Chang, I. C.; Chang, Y.-C.; Chen, Y.-L.; Lin, I. N.; Chiu, H.-T.; Lee, C.-Y. The “Cascade Effect” of Nano/Micro Hierarchical Structure: A New Concept for Designing the High Photoactivity Materials – an Example for  $\text{TiO}_2$ . *Appl. Catal., B* **2013**, *142–143*, 752–760.
- (106) Li, X.; Fan, T.; Zhou, H.; Chow, S.-K.; Zhang, W.; Zhang, D.; Guo, Q.; Ogawa, H. Enhanced Light-Harvesting and Photocatalytic Properties in Morph- $\text{TiO}_2$  from Green-Leaf Biotemplates. *Adv. Funct. Mater.* **2009**, *19*, 45–56.
- (107) Yun, H. J.; Lee, H.; Kim, N. D.; Lee, D. M.; Yu, S.; Yi, J. A Combination of Two Visible-Light Responsive Photocatalysts for Achieving the Z-Scheme in the Solid State. *ACS Nano* **2011**, *5*, 4084–4090.
- (108) Tada, H.; Mitsui, T.; Kiyonaga, T.; Akita, T.; Tanaka, K. All-Solid-State Z-Scheme in  $\text{CdS-Au-TiO}_2$  Three-Component Nano-junction System. *Nat. Mater.* **2006**, *5*, 782–786.